Precision constrained stochastic resonance in a feed forward neural network

Nhamoinesu Mtetwa and Leslie S. Smith

Department of Computing Science, University of Stirling

Stirling FK9 4LA, UK

corresponding author: Nhamoinesu Mtetwa, email: nmt@cs.stir.ac.uk,

tel +44 (0) 1786 467457, Fax +44 (0) 1786 464551

***Abstract*— Stochastic resonance (SR) is a phenomenon in which the response of a nonlinear system to a subthreshold information-bearing signal is optimised by the presence of noise. By considering a nonlinear system (network of leaky integrate-and-fire (LIF) neurons) that captures the functional dynamics of neuronal firing, we demonstrate that sensory neurons could, in principle harness SR to optimise the detection and transmission of weak stimuli. We have previously characterised this effect by use of signal-to-noise ratio (SNR). Here in addition to SNR, we apply an entropy-based measure (Fisher information) and compare the two measures of quantifying SR. We also discuss the performance of these two SR measures in a full precision floating point model simulated in Java and in a precision limited integer model simulated on a Field Programmable Gate Array (FPGA). We report in this study that stochastic resonance which is mainly associated with floating point implementations is possible in both a single LIF neuron and a network of LIF neurons implemented on lower resolution integer based digital hardware. We also report that such a network can improve the SNR and Fisher information of the output over a single LIF neuron.**

***Index Terms*— Stochastic resonance (SR), signal-to-noise ratio (SNR), Fisher information, limited resolution, leaky integrate-and-fire (LIF).**

I. Introduction

The focus of this work is on implementing neuronal SR on reduced resolution digital hardware using an integer model. By implementing neuronal SR on a precision-constrained digital platform of the Field Programmable Gate Array (FPGA) type we aim to bring neuronal modelling closer to its application in prosthetic devices like hearing aids. Floating point realisation would require either expensive Application Specific Integrated Circuits (ASICs) or huge FPGAs.

Stochastic resonance is said to occur when a bistable nonlinear system is driven by a weak periodic signal, and provision of additional noise improves the system's detection of the periodic signal (see [18] for a review). Here "weak" means that the input signal is so small that when applied alone it is undetected [39]. The resonance effect arises through the conjunction of two competing mechanisms: the noise-induced linearisation (dithering) of the model's firing rate and the increase in the variability of the number of spikes in the output. Experimentally, SR was first demonstrated with a noise driven circuit known as a Schmitt trigger [17]. It took several years before the interest of physicists (who have done most of the theoretical analysis) ignited, sparked by the demonstration of SR in a bistable ring-laser experiment [49]. Now SR has crossed disciplinary boundaries: its role in sensory biology has been explored in experiments on single crayfish neurons [16], cat visual cortex [1], cricket cercal sensory system [30], human memory retrieval [48], human visual perception [36], [51] and human hearing [54], [26], [24].

Since its introduction, SR has been shown to occur under many different circumstances, with various types of signals, nonlinear processes, and measures of performance [12], [19], [25], [9], [8], [35], [32]. Most of the literature on SR involves a signal which is itself too weak to elicit a strong response from the nonlinear system. For larger (suprathreshold) signals, SR induced by a single nonlinearity disappears [7], [30]. However it has recently been shown that suprathreshold SR can occur in an array of parallel nonlinear units with independent noise injection where their outputs are summed [21], [45], [46]. Like subthreshold SR, there is an optimal nonzero noise level. The increase in output entropy improves the independence in information transmitted by individual units, giving rise to a net increase in transmitted information, under optimal noise conditions. However, suprathreshold SR cannot be measured using SNR [47].

While we recognise the importance of suprathreshold SR, this study will only focus on subthreshold SR in neuronal systems for the following reasons. Firstly, we are interested in SR in both single input layer LIF neurons and output layer LIF neuron (see figure 1). Secondly we also want to quantify SR using SNR which we cannot do for suprathreshold SR as already discussed. Specifically we study SR in a parallel array of LIF neurons receiving a common subthreshold signal with an alpha synapse [42] at the output. Similar studies have been done by among others [34], [23] who looked at enhanced information transmission in an array of comparators. [43] looked at a parallel array of LIF neurons which just sums the output while [53] looked at a similar architecture with a depressing synapse at the output LIF neuron.

Simulation of SR in "continuous" systems using floating point based models is well established [5], [49] and [44]. Such models are fairly accurate but do not always result in real-time performance. This work aims to show that SR still occurs with lower resolution integer based representations which allow real-time performance on inexpensive digital hardware such as FPGAs. FPGAs are reconfigurable programmable logic devices [6].

We investigate the effect of varying the resolution of the numbers inside the simulation of SR in a feed forward neural network (see figure 1): we do this by examining SR in a 32 bit floating point model of this system implemented in Java, and in an integer model where the integer length is varied downwards from 16 bits implemented on the FPGA. The SR effect is assessed by applying a subthreshold periodic signal plus noise to the system, and examining its output in terms of SNR and Fisher information. For both models we calculate the SNR and the Fisher information at different input noise amplitudes. For the integer model, besides varying the noise, we also calculate the SNR and Fisher information values at different resolutions. This work extends our previous work in [38], [37] related to digital implementation of real-time neural sensory systems for signal detection in noisy inputs. The input layer neurons (see figure 1) depict SR in a single neuron receiving noisy continuous stimulation while the output neuron, stimulated by spikes from the input neurons, depicts SR in a network. Our results show that integer lengths of at least 10 bits produce usable results, and that the network produces a performance improvement for 6 input neurons at integer length of at least 11 bits using the SNR measure but not with the Fisher information measure. The Fisher information measure requires more than 6 input neurons to register an improvement over the input at the output.

A. Measuring stochastic resonance

Stochastic resonance can be demonstrated using almost any method of detecting or reconstructing a subthreshold signal from information contained in the crossings of the threshold θ of a detector by the signal plus noise. SR metrics are chosen according to the nature of the input signals and of the transmission system itself. If the signal is periodic and observed over a relatively long time interval, then it is common to do a Fourier analysis of the crossing times and to measure the information thus gained about the signal as the ratio of the power spectral density (PSD) at the signal frequency to that generated by noise at the nearby frequencies (the signal-to-noise ratio see equation 1) [49].

$$\mathrm{SNR} = \frac{\mathrm{PSD}_{f_{\mathrm{sig}}}}{\mathrm{PSD}_{f_{\mathrm{other}}}} \tag{1}$$

where f_{sig} is the signal frequency and f_{other} is the frequency bands outside the signal frequency. Another way to quantify the SR effect, related to the way neural activity is analysed, is to investigate the (empirical) residence-time probability distribution, or interspike interval histogram [31]. If an aperiodic signal is observed over a relatively long time interval, then goodness of signal reconstruction or the coherence between the signal and the output has been measured by a correlation measure [11] and entropy based methods [18].

SR is characterised by improving the measure of depen-

dence of the output on the input by means of an increase in the level of noise. The standard measure of SR has been the SNR of the power spectrum [49]. All spectral quantities, including the SNR, are based on averages over long times. A feature present on average, however, is not necessarily present in a limited sample, such as the record of a single neuron's spike train over the first few hundred milliseconds of its response. Thus the SNR does not in any way address whether the system can reliably perform signal detection based on the spike output of a single neuron over a short duration. More appropriate measures that explicitly depend on the sampling time are ones based on information theory [22], [44]. In this paper we will examine the existence of stochastic resonance in SNR (see equation 1) and in an information theoretic measure using the leaky integrate-and-fire neuron model.

The information theoretic measure that we use is the Fisher information, $J(\mu)$ normally defined as [14]:

$$J(\mu) = \int \frac{1}{p(N;\mu)} \big(\frac{\partial}{\partial \mu} p(N;\mu)\big)^2 dN \tag{2}$$

where $p(N;\mu)$ is the probability of observing N spikes, given an input μ. The Fisher information is closely related to the entropy, or inherent uncertainty, in the distribution $p(N;\mu)$. The Fisher information can also be interpreted as the amount of information in the output about the input signal [41]. Maximising the entropy subject to a fixed parameter is equivalent to minimising the Fisher information about that parameter. If the input noise amplitude is fixed, then μ is the only free parameter of the spike count distribution. Using these facts, it is possible to write down a simple lower bound for the Fisher information [44]:

$$J_{LB}(\mu) = \frac{1}{{\sigma^2}_N(\mu)} \Big(\frac{\partial \mu_N}{\partial \mu}\Big)^2 \tag{3}$$

where σ_N and μ_N are the standard deviation and mean of the spike count probability distribution, respectively.

Since the spike count μ_N over a fixed window of time is an estimate of the firing rate $f(\mu)$, we can rewrite the lower bound of the Fisher information from (3) as [44]:

$$J_{LB}(\mu) = \frac{1}{{\sigma^2}_{f(\mu)}} \Big[\frac{\partial}{\partial \mu} \langle f(\mu) \rangle\Big]^2 \tag{4}$$

where $\langle . \rangle$ denotes averaging. Recent work on the use of information theoretic measures to characterise stochastic resonance in a neural arrays can be found in the works of [47], [34], [23], [40].

II. The Model

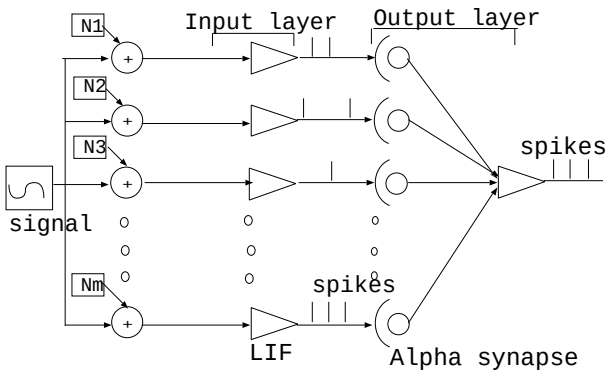

Fig. 1. Network model. Layer 1: m identical, input LIF neurons receive the same 20Hz subthreshold sinusoidal input plus independent uncorrelated noise (N1, N2, N3, ..., Nm). Output: Similar LIF neuron model receives spiking input via m Alpha synapses.

Each LIF neuron in figure 1 is modelled by the LIF neuron model equation (5) which idealises the point neuron membrane as a capacitor C, in parallel with a resistor of resistance R. The effective current $I(t)$ may hyperpolarise or depolarise the

membrane.

$$C\frac{dV}{dt} = I(t) - \frac{V(t)}{R} \tag{5}$$

For the input neurons, $I(t)$ is composed of a periodic sub-threshold sinusoidal part and a stochastic component. This component is the additive noise $\xi_i(t)$ [4], different for each input neuron. It was generated by bandpassing Gaussian white noise (see below). For the output neuron

$$I(t) = a\sum_{k=1}^{N} I_k(t) \tag{6}$$

where a is the synaptic weight (determined by looking at weights which maximise SNR as explained later) which is the same for all the neurons and

$$I_k(t) = \sum_{i=1}^{m} \alpha(t - t_{ki}) \tag{7}$$

where the index $k = 1, ..., N$ denotes the input neurons and the index *i* denotes the i^{th} input from a particular input neuron k, whose time of arrival is $t_{k_i}(0 < t_{k_1} < t_{k_2} < ... < t_{k_m})$ and m is the number of active spikes from input neuron k. The alpha function is given by [28]:

$$\alpha(t) = \frac{1}{\tau_s}e^{-\frac{t}{\tau_s}} \quad \text{for} \quad t \geq 0, \quad \text{and} \quad 0 \quad \text{for} \quad t < 0. \tag{8}$$

where τ_s is the synaptic time constant for synapse k in the millisecond range.

The synaptic weight a was determined as follows. The network was run with one neuron and the maximum SNR value, $SNR_{\max}$ was determined from the SNR versus noise plot. The noise strength $\sigma_{\max}$ which resulted in $SNR_{\max}$ was also noted. The network was then run with one input and one output neuron keeping the noise value at $\sigma_{\max}$, the value that gave us the maximum SNR value for the single neuron case. The synaptic weight was changed until the SNR value for the output neuron equalled the maximum value for the single neuron case. The resulting synaptic weight W (which equalises the SNR at the output with $SNR_{\max}$) was then divided by the number of coincident spikes needed to make the output neuron fire a single spike with a weight of 1. That is, the synaptic weight a for all the synapses is given by: $a = \frac{W}{n}$. The rationale behind this synaptic weight was to ensure that the coupling between the input neurons and the output neuron is weak, that is, a single spike from an input neuron in a multiple neuron network does not cause a spike on the output neuron. Coupling is said to be strong if each spike from the input neurons causes a spike on the output neuron. According to the results reported by [53] stochastic resonance was stronger for weaker coupling between input neurons and the output neuron than for stronger coupling.

An alpha synapse was used in preference to a step function for both biological and engineering plausibility. The rise time of the alpha synapse was 10 ms. A network model similar to ours using a depressing synapse with 4 input layer neurons was studied in [53]. They report that a depressing synapse improves the SNR at the output. Similar results were also reported in [13] using a rate coding based FitzHugh-Nagumo model network with a similar topology. Both these networks used floating point numbers.

The network was simulated using a 1 ms time step. For the input neurons, the noise, $\xi_i(t)$ was generated from a discrete noise signal in which the value at each time step was a sample from N(0,1), the Gaussian distribution with

mean 0 and variance 1 by bandapassing it between 5 and 100 Hz. This $\xi_i(t)$ varies relatively little between adjacent samples. The value of τ_s in the alpha function (equation 8) is also such that the inputs to the output neuron also vary relatively little between adjacent samples. It is therefore valid to use a simple Euler approximation otherwise techniques for numerically solving stochastic differential equations like the one described by [33], [27] would have to be used.

The floating point model uses the Euler approximation of equation (5) given by equation (9) .

$$V(t+\Delta t) = V(t)(1-\frac{\Delta t}{\tau}) + \Delta t I(t) \tag{9}$$

where Δt is the time step, and $\tau = CR$ is the membrane time constant.

Equation (9) is implemented on an FPGA platform by (i) making all values integers and (ii) making division only by powers of 2. $\frac{\Delta t}{\tau}$ is expressed as 2^{-k} (we call k the leakage factor) and Δt is expressed as 2^{-m}. This is because full integer division is expensive to implement (both in number of gates and speed) whereas bit-shifting is very fast. The alpha function was implemented using a look-up table. In integer form equation (9) becomes

$$\bar{V}(t+1) \approx \bar{V}(t) - \bar{V}(t) >> k + \bar{I}(t) >> m \tag{10}$$

where $>>$ denotes bit-shifting to the right which is basically division in powers of 2.

III. Methodology

The floating point model can take inputs directly from $I(t)$. However the integer model requires integer inputs which means the input signals must be quantised. This is achieved by multiplying the input signals by 2^n (where n is the resolution i.e. integer length). The floating point model was implemented in Java and the integer model in Handel-C [2]. The output spike trains for several runs with different noise streams each time were collected for the floating point model and different integer lengths (10, 11, 12 and 16 bits) for the integer model on the FPGA. The main output of interest are the spike trains from both the "input" and "output" neurons (see figure 1) from which the two SR metrics were computed using Matlab.

A. SNR

The power spectra were computed using the method of Gabbiani and Koch in chapter 9 of [29]. The SNR is then computed from the power spectra using the method of Chapeau-Blondeau in [10]:

$$\mathrm{SNR} = \frac{S(\omega)}{N(\omega)} \tag{11}$$

where $S(\omega)$ is the power spectrum of the spike train at the signal frequency and $N(\omega)$ is the power spectrum of the background noise around the signal frequency. Each SNR value is an average from 10 different spike trains each 4 096 samples long.

B. Fisher information

Standard practice in neurophysiology consists of quantifying the neuronal response by summing up the number of spikes fired by a neuron over a fixed time period. The spike count constitutes an estimate of the firing rate of the neuron. Once a threshold of a neuron is fixed and set to a detection criterion, it can act as a detector of the spike signal from a presynaptic sensory neuron. Consequently, the spike count is

the natural measure for a signal detection system made out of neuronal building blocks [44]. Because we are dealing with a sinusoidal signal we imagine that the periodic component of the LIF unit's spike train is determined by the average number of spikes fired during the "up" phase of the sinusoid after subtracting the number of spikes fired during the "down" phase. The length of the window for determining the firing rate is equivalent to half the period of the sinusoidal input signal.

The Fisher information (lower bound) is computed as follows: from equation 4 we approximate the partial derivative:

$$\frac{\partial}{\partial \mu}\langle f(\mu)\rangle \tag{12}$$

by

$$\Big[\frac{\langle f(\mu_1)\rangle - \langle f(\mu_2)\rangle}{\langle \mu_1\rangle - \langle \mu_2\rangle}\Big] \tag{13}$$

where $\langle f(\mu_1)\rangle$ is the mean firing rate for the first half of the input signal period and $\langle f(\mu_2)\rangle$ is the mean firing rate for the second half of the input signal period. $\langle \mu_1\rangle$ is the mean of the first half of the input signal and $\langle \mu_2\rangle$ is the mean of the second half of the input signal.

Therefore the Fisher information (lower bound) is given by:

$$J_{LB}(\mu) = \frac{1}{{\sigma^2}_{f(\mu)}}\Big[\frac{\langle f(\mu_1)\rangle - \langle f(\mu_2)\rangle}{\langle \mu_1\rangle - \langle \mu_2\rangle}\Big]^2 \tag{14}$$

IV. Results

The FPGA used here is a Xilinx Virtex XCV1000 [52]. A 7-neuron network implementation on this FPGA occupied 147 625 gates and a single neuron implementation occupied 10 718 gates [38]. The results presented here are for the following network and signal parameters:

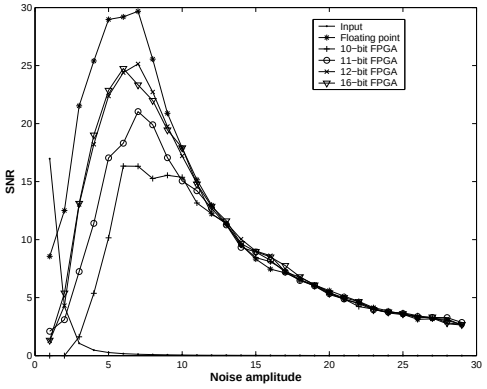

Fig. 2. Input layer neuron SNR for Java (floating point) and FPGA (integer resolutions 10,11,12 and 16).

- membrane time constant τ = 20ms;
- threshold θ = 20mV;
- signal frequency ω = 20Hz;
- absolute refractory period = 10ms;
- synaptic time constant = 10ms;
- Bandpassed noise $\xi_i(t)$, of variable amplitude;
- spike trains were 4 096 samples long.

The choice of parameters was motivated by the applicability of the network topology to auditory signal processing and the frequency regimes in which stochastic resonance has been well studied according to literature. Stochastic resonance is well established in the low frequency regime according to [18] and [50]. Hence the choice of the 20Hz frequency. LIF neurons model real neurons which operate on continuous time-varying

signals and the choice of time constants must match those of the signals. The membrane time constant τ was motivated by measurements from real neurons and the choice of frequency and also its possible role for sound segregation in auditory scene analysis [20]. The absolute refractory period t_{ref} was chosen based on values reported in the literature on neuronal modelling [15]. t_{ref} sets the limit for the firing frequency of the neuron, the neuron can not fire beyond $\frac{1}{t_{\mathrm{ref}}}$ Hz.

A. SNR

The results are summarised in figures 2 to 13. They show that there is stochastic resonance in the input neurons and the output neuron in both models using both the SNR and the Fisher information metrics.

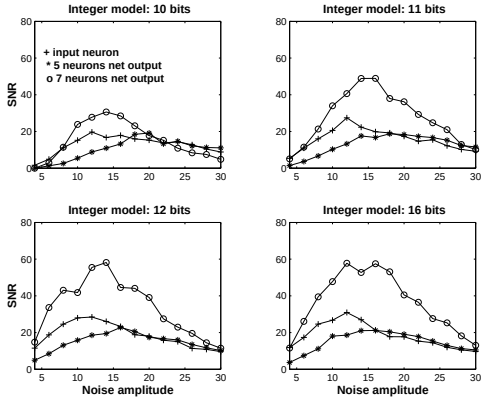

Fig. 3. FPGA (resolutions 10,11,12 and 16) input layer neuron and output layer neuron SNRs for the 5- and 7-neuron network.

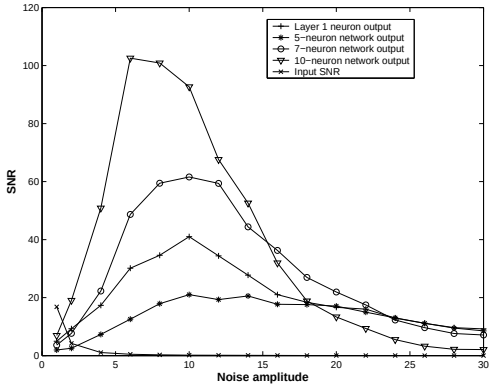

Fig. 4. Java 5-, 7- and 10-neuron network input layer neuron and output layer neuron SNR

Figure 2 shows that at the input layer, Java SNR values are better than all the FPGA resolutions considered. It also shows that SNR values for the integer model improve for resolutions up to 12 bits after which they stay constant as evidenced by the similarity between SNR values for 12 bits and 16 bits resolutions.

The SNR at the output also increases with increase in resolution (see figures 5 and 6) just like it does at the input layer. In both figures the SNR values for the integer model resolutions of 12 and 16 bits slightly overtake the Java SNR between noise amplitudes of 10 and 15. This is interesting because at the input layer SNR values for the Java model are always better than at all the FPGA resolutions considered (see figure 2).

Figure 3 shows that the SNR at the output neuron is influenced by both the resolution and number of input neurons. The SNR value at the output increases with an increase in the number of input neurons. The 10-bit resolution SNR result shows that the input layer SNR is always better than the output neuron result for both 5- and 7-neuron networks. For 11 bits, 12 bits and 16 bits, only the output for the 5-neuron network is less than the input layer neuron SNR, the output neuron SNR for the 7-neuron network is always above the input layer for all the noise values considered. This suggests there is an interaction between the output neuron SNR, the number of input neurons and the resolution of the integer model.

Figure 4 shows that as the network increases in size so does the SNR of the output neuron. This result was only proven on a limited scale on the FPGA (see figure 3) because we were unable to produce a network with more than 7 neurons due to computing equipment limitations.

B. Fisher information

The floating point and integer single input neuron spike train Fisher information exhibit the familiar shape of stochastic resonance (see figure 7). The general shape of the Fisher information curves for both the floating point model and all the resolutions on the integer model portray stochastic resonance, (see figure 8). At the low noise end, the graphs are quite separated and it is clear that the Fisher information values increase with resolution with the 10 bits integer being lowest and 32 bits floating point being highest. The 12 and 16 bits graphs are almost indistinguishable throughout. The effect of quantisation is stronger at the lower noise end as shown by the graphs being clearly separated while at the high noise end the graphs are lumped together because noise is the dominant feature at this end.

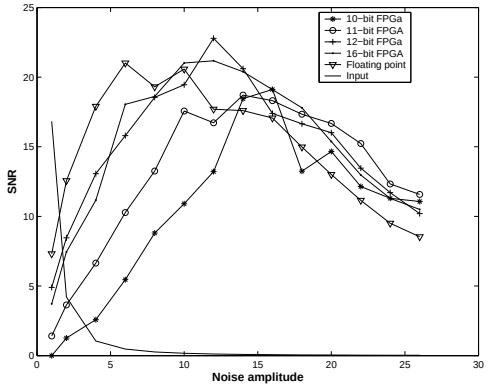

Fig. 5. 5-neuron network output layer neuron SNR for both Java and FPGA (resolutions 10, 11, 12 and 16).

At the output neuron the curves are much more separated as seen in figure 9. 10 bits integer is well below all the other resolutions. The graphs can still be separated on resolutions though. 12 and 16 bits actually out-perform the 32 bits floating point model for most of the noise amplitudes considered.

As the network size increases we see that the higher resolutions dominate (16 bits integer and 32 bits floating point), see figure 10. This suggests that there is an interaction between network size and the resolution.

In the integer model, for the network sizes considered (5 and 7-neuron network) the output neuron Fisher information

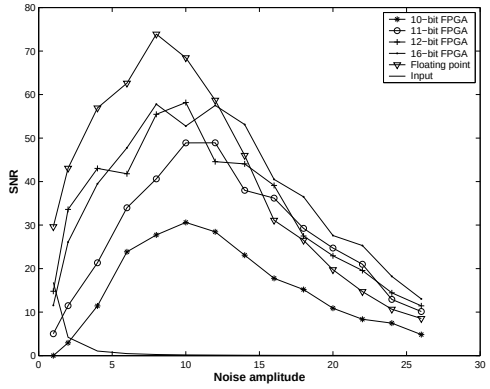

Fig. 6. 7-neuron network output layer neuron SNR for both Java and FPGA (resolutions 10,11,12 and 16).

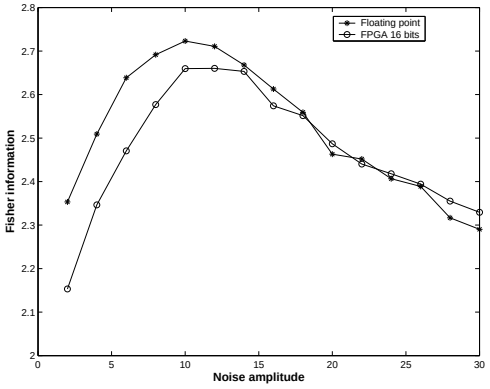

Fig. 7. Input layer neuron Fisher information for both floating point and integer models.

never exceeds the input neuron Fisher information for all the resolutions considered (10, 11, 12 and 16 bits), see figure 11. However, the gap between the input Fisher information and output Fisher information decreases as the network size is increased. The narrowing of the gap between the output neuron Fisher information and the input neuron Fisher information is resolution dependent. The gap between the input neuron Fisher information and 7-neuron network out Fisher information is biggest at 10 bits and smallest at 16 bits. The difference between the 5-neuron and 7-neuron output is also resolution dependent. In the 10 bits case, 7-neuron network output is less than 5-neuron network output for the lower noise values where as for 16 bits the 7-neuron network output is above the 5-neuron network for all the noise amplitudes considered as can be seen in figure 11.

The input neuron does not appear to be affected much by resolution because it peaks around a Fisher information value of 2.6 for all the resolutions considered (figures 11 and 12).

Both SR measures have shown that they can portray stochastic resonance in both the integer and floating point models both at single and network level.

Due to computational limitations we were not able to get a network of size bigger than 7 neurons on the FPGA but we were able to do that with the floating point model in Java. Increasing the number of neurons to 10 and beyond showed that the Fisher information of the output neuron actually exceeds that of the input neuron as shown in figure 12.

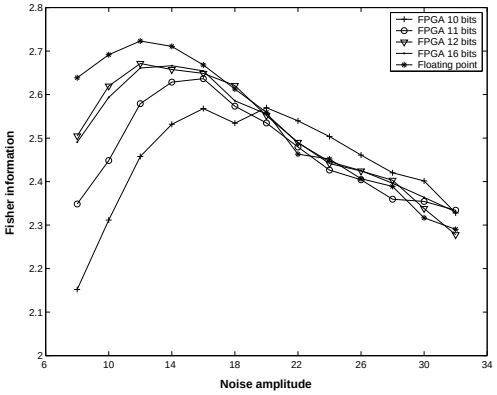

Fig. 8. Effect of resolution on a single input layer neuron Fisher information.

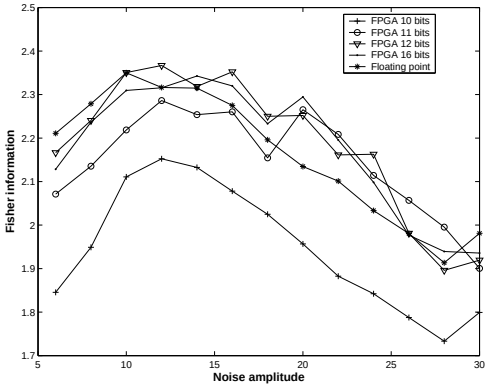

Fig. 9. 5-neuron network output layer Fisher information for both floating point and integer models.

V. Discussion

The results presented above are influenced by precision limitation (quantisation), network size and the type of SR metric used.

A. Quantisation

Quantisation affects the evolution of activation and its effect is that the changes in $V(t)$ over Δt implemented by equation (10) are forced into integer values and that the integer activation value ceases to decrease when $(V(t) >> k + I(t) >> m) < 1$ resulting in the LIF neuron not decaying to zero from a high start value with no input, see figure 13. This leakage problem in the integer model is also coupled to the size of the time step Δt. Decreasing the time step makes the problem worse as the decrement $\frac{V(t)\times\Delta t}{\tau}$, is proportional to Δt. Yet increasing Δt is not normally an option, as we need $\Delta t \ll T$. For the chosen values of $\tau = 0.02s$ and $\Delta t = 0.001s$, the resolution needs to be at least 10 bits.

B. Stochastic resonance

Armed with the expressions for signal and noise spectra, we can write $SNR = S(\omega)/N(\omega)$. The increase in the signal power due to stochastic linearisation is counteracted by the increase in the noise power. The LIF system takes the incoherent energy from the noise and feeds it into coherent energy at the frequency of the periodic signal leading to an increase in the SNR at the output. The uncorrelated noise increases only by a factor of $\sqrt{N}$ on average across the population of the neurons, while the coherent input signal is

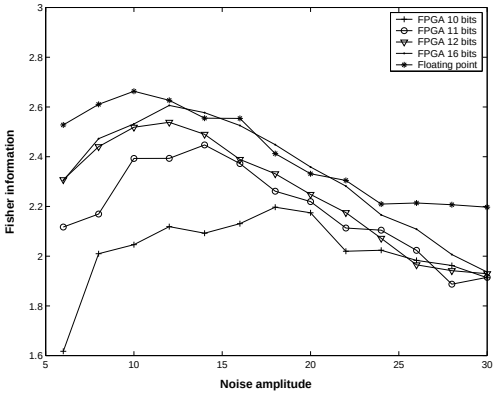

Fig. 10. 7-neuron network output layer Fisher information for both floating point and integer models.

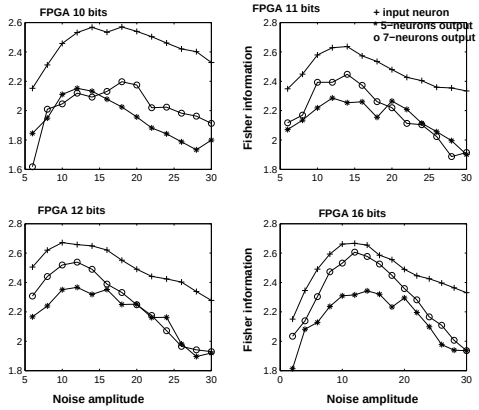

Fig. 11. Interaction between network size and resolution for the integer model (10, 11, 12 and 16 bits). This figure compares the output layer neuron Fisher information for different network sizes and resolutions with that of a single input layer neuron.

strengthened by a factor of N. This yields an increased SNR and a more sensitive neural network.

Figures 2, 4, 3, 5 and 6 show that the differences in SNR values for the resolutions considered in the low noise regime are much higher than the differences at the high noise end. This applies to both input and output neurons. The difference in SNR in the lower noise levels at the input layer (see figure 2) are as much as 3dB and the same differences for the output layer are as much 6dB (see figure 6). The decrease in the differences in SNR (as noise strength is increased) may suggest that quantisation effects are more pronounced at lower signal plus noise levels. This could be attributed to loss of changes in the activation. The maximum input layer improvement in SNR due to SR on the FPGA platform never reaches the same level as that of the floating point model for lower noise levels.

For the integrate-and-fire model, SR in the Fisher information $J(\mu)$ arises through the conjunction of two effects: stochastic linearisation - the increase in the slope of the firing rate curve - and the noise-induced increase in the spike count variance. Adding noise to the input comes with a price: the noise in the output increases as well. Thus an increase in the separation in mean firing does not imply an increase in the discriminability or the Fisher information. Looking at equation 4, we note that the numerator is affected by stochastic linearisation, whereas the denominator measures the “noise”

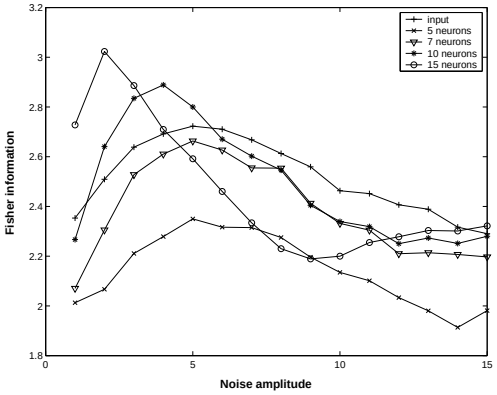

Fig. 12. Floating point model Fisher information for different network sizes. The figure compares the output layer neuron Fisher information for different sizes with that of a single input layer neuron. It shows that the output layer neuron Fisher information for network sizes greater than 7 exceeds that of the input layer neurons.

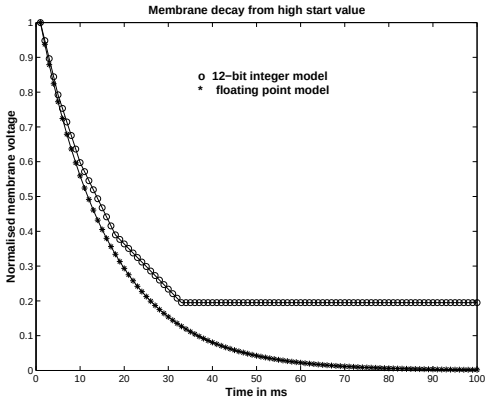

Fig. 13. Membrane decay due to leakage from a high start value in the absence of input.

in the output. For the LIF neuron model, both numerator and denominator always increase as a function of the input noise; eventually, though, the denominator will dominate. As a consequence, the Fisher information will first rise and then fall as a function of the input noise variance; this is the origin of the SR peak.

C. Comparison between the two metrics

The results presented in the previous section have shown that the SR effect can be measured using SNR and Fisher information metrics. Both SR measures are sensitive to resolution. At the input neuron both metrics respond similarly to changes in resolution in that the lowest resolution (10 bits) has the lowest metric value and the highest resolution (32 bits) has the highest metric value (see figures 2 (SNR) and 8 (Fisher information)). 12 and 16 bits resolution are indistinguishable for both SNR and Fisher information at the input neuron. Both measures are affected in a similar way by quantisation in that the graphs for both metrics are separated at low noise values but lumped together at high noise values for the input neuron. At network level the main similarity is that the curves for both metrics are more separated at the high noise end than at the input neuron for the same noise values, see figures 5, 6 (SNR) and 9, 10 (Fisher information).

The main difference between the two measures is at network level. When we compare the input neurons and the output

neuron for different network sizes we see that the output SNR of the 7-neuron network exceeds the input neuron SNR for resolutions above 10 bits. On the contrary the 7-neuron network output Fisher information never exceeds that of the input neuron Fisher information. However, as the number of neurons is increased to 10 neurons the output Fisher information does exceed that of the input neuron but this result was only proven for the floating point model. We think the explanation for this lies in the way the two metrics are computed. The Fisher information has the term ${\sigma^2}_{f(\mu)}$ in its denominator which is a noise measure for the entire spike train which scales with $\sqrt{N}$. This means as the number of neurons increases we are dividing by a smaller number each time. On the other hand the SNR is computed by dividing by noise power in the vicinity of the signal frequency.

Collins showed, in a summing network of identical Fitzhugh-Nagumo model neurons, that an emergent property of SR in multicomponent systems is that the enhancement of the response becomes independent of the exact value of the noise variance. This allows networks of elements with finite precision to take advantage of SR for diverse inputs.

VI. Conclusion

The conditions we have presented, of various forms of noise-enhanced transmission with information-theoretic characterisations, are merely illustrative. The effect is preserved over a broad range of signals and nonlinear systems, as it was verified to be the case in studies on other forms of stochastic resonance [3]. Also different measures can be used to quantify a stochastic resonance effect, especially measures from information theory as we have shown here, all depending on the purpose and prospect involved.

Stochastic resonance remains an emerging effect. From a conceptual standpoint, stochastic resonance is an important phenomenon as it modifies the status of noise by establishing that in nonlinear systems noise is not necessarily a nuisance but may sometimes be turned into a benefit. From a practical standpoint, stochastic resonance may have useful applications for signal processing by nonlinear systems, especially when no full control is available over nonlinearities. Both aspects of stochastic resonance call for further exploration.

We have shown that a network of low-precision LIF neurons can take advantage of stochastic resonance to accurately encode and transmit an input. The collective properties of these systems exceed the limitations of a single element. Careful tuning of properties of the elements, such as thresholds, may yield further improvements in the performance of the system. This is important because such systems can permit digital electronic implementation with real-time performance, for example through FPGA implementations. The amount of SR may not be as high as in high resolution implementations. It has also been shown that in integer systems SNR saturates as we increase the bit length at which activation is computed. For the parameters chosen in this simulation, SNR was not found to improve with an increase in the resolution beyond 12 bits for input neurons. The output neuron saturates at a resolution higher than 12 bits. The improvement in output SNR when the output of a parallel array of neurons converge on one neuron could justify the existence of such networks in the central

nervous system confirming the findings of [13].

In terms of application, this work could be used in the design of digital front-end systems for implantable visual and cochlear prostheses [47] or for detecting regularities in noisy inputs in highly sensitive input devices. This work could be extended to suprathreshold signals and investigate the effect of precision limitation on this type of SR using an information theoretic measure.

ACKNOWLEDGEMENTS

The authors gratefully acknowledge the help and advice of B. Graham, D. McLean and A. Hussain. N. Mtetwa would like to thank the University of Stirling for funding his PhD under which most of this work was done.

REFERENCES

[1] J.S. Anderson, I. Lampl, D.C. Gillespie, and D. Ferster. The contribution of noise to contrast invariance of orientation tuning in cat visual cortex. *Science*, 290:1968–1972, 2000.

[2] M. Aubury, I. Page, G. Randall, J. Saul, and R. Watts. *Handel-C language reference guide*. Oxford University, Oxford University computing laboratory, August 28 1996.

[3] M.J. Barber and B.K. Dellen. Noise-induced signal enhancement in heterogeneous neural networks. In *Computational science - ICCS 2001: International conference*, pages 996–1000, San Francisco, CA, USA, 2001. Springer-Verlag Heidelberg.

[4] M. Barbi, S. Chillemi, and A.D. Garbo. The leaky integrate-and-fire neuron: a useful tool to investigate SR. *Chaos, solutions and fractals*, pages 1273–1275, 2000.

[5] R. Benzi, G. Parisi, A. Sutera, and A. Vulpiani. Stochastic resonance in climatic changes. *Tellus*, 34:10–16, 1982.

[6] G. Bostock. *FPGAs and Programmable LSI*. Butterworth Heinemann, 1996.

[7] A.R. Bulsara and A. Zador. Threshold detection of wideband signals: A noise induced maximum in the mutual information. *Phys Rev E*, 54(2185), 1996.

[8] F. Chapeau-Blondeau. Noise-enhanced capacity via stochastic resonance in asymmetric binary channel. *Phys Rev E*, 55(2016), 1997.

[9] F. Chapeau-Blondeau and X. Godivier. The theory of stochastic resonance in signal transmission by static non-linear systems. *Phhys. Rev. E*, 55:1478–1495, 1997.

[10] F. Chapeau-Blondeau, X. Godivier, and N. Chambet. Stochastic resonance in a neuronal model that transmits spike trains. *Physical Review E*, 53:1273–1275, 1996.

[11] J.J. Collins, C.C. Chow, A.C. Capela, and T. T. Imhoff. Aperiodic stochastic resonance. *Phys. Rev. E*, 54:5575–5584, 1996.

[12] J.J. Collins, C.C. Chow, and T.T. Imhoff. Aperiodic stochastic resonance in excitable systems. *Phys Rev E*, 52, 1995.

[13] J.J. Collins, C.C. Chow, and T.T. Imhoff. Aperiodic stochastic resonance in excitable systems. *Phys. Rev. E*, 52:3321–3324, 1995.

[14] T.M. Cover and J.A Thomas. *Elements of information theory*. New York: Wiley-Interscience, 1991.

[15] P. Dayan and L.F. Abbott. *Theoretical neuroscience: computational and mathematical modeling of neural systems*. The MIT Press, 2001.

[16] J.K. Douglas, L. Wilkens, E. Pantazelou, and F. Moss. Noise enhancement of information transfer in crayfish mechanoreceptor by stochastic resonance. *Nature*, 365:337–340, 1993.

[17] S. Fauve and F. Heslot. Stochastic resonance in a bistable system. *Phys. Lett.*, 97A:5–7, 1983.

[18] L. Gammaitoni, P. Hanggi, P. Jung, and P. Marchesoni. Stochastic resonance. *Review Modern Physics*, 70:223–287, 1998.

[19] Z. Gingl, L.B. Kiss, and F. Moss. Non-dynamical stochastic resonance: Theory and experiments with white and various coloured noise. *Europhys Lett*, 29(191), 1995.

[20] M.A. Glover, A. Hamilton, and L.S. Smith. Analogue VLSI leaky integrate-and-fire neurons and their use in a sound analysis system. *Analog Integrated Circuits and Signal Processing, Special Issue: Microelectronics for Bio-inspired Systems (Selected Papers from MicroNeuro'99 Conference)*, 30(2):91–100, 1999.

[21] G.P. Harmer and D. Abbott. Motion detection and stochastic resonance in noisy environments. *Microeletr J*, 32(12):959–967, 2001.

[22] C. Heneghan, C.C. Chow, J.J. Collins, T.T. Imhoff, Lowen, S.B., and M.C. Teich. Information measure quantifying aperiodic stochastic resonance. *Phys. Rev. E.*, 54:R2228–R2231, 1996.

[23] T. Hoch, G. Wenning, and K. Obermayer. Adaptation using local information for maximizing the global cost. *Neurocomputing*, 52-4:541–546, 2003.

[24] N. Hohn and A. N. Burkitt. Modelling the neural response to speech: stochastic resonance and coding of vowel-like stimuli. In *IEEE EMBS Conference*, MOnash University, 2001.

[25] M.E. Inchiosa and A.R. Bulsara. Signal detection statistics for stochastic resonators. *Phys Rev E*, 53(2021), 1996.

[26] F. Jaramillo and K. Weisenfeld. Physiologocal noise enhances mechanoelectrical trasduction in hair cells. *Chaos, Solutions and Fractals*, 2000.

[27] P. E. Kloeden, E. Platen, and H. Schurz. *Numerical solution of SDE through computer experiments*. Springer, 1997.

[28] C. Koch. *Biophysics of Computation*. Oxford University Press, NY, 1999.

[29] C. Koch and I. Segev, editors. *Methods in Neural modeling: from ions to networks*. The MIT Press, second edition, 1999.

[30] J.E. Levin and J.P. Miller. Broadband neural encoding in the cricket cercal sensory system enhanced by stochastic resonance. *Nature*, 380:165–168, 1996.

[31] A. Longtin, A. Bulsara, and F. Moss. Time-interval sequences in bistable systems and noise-induced transmission of information by sensory neurons. *Phys. Rev Lett.*, 67:656–659, 1991.

[32] D.G. Luchinsky, P.V.E. McClintock R. Mannella, and N.G. Stocks. Stochastic resonance in electrical circuits II. nonconventional stochastic resonance. *IEEE Trans. Circuits and Systems*, 46:1215–1224, 1999.

[33] R. Mannela and V. Palleschi. Fast and precise algorithm for computer simulation of stochastic differential equations. *Physical Review A*, 40:3381–3386, 1989.

[34] M.D. McDonnell, D. Abbott, and C.E.M. Pearce. An analysis of noise enhanced information transmission in an array of comparators. *Microeletr J*, 33(12):1079–1089, 2002.

[35] S. Mitaim and B. Kosko. Adaptive stochastic resonance. *Proceedings of the IEEE: special issue on intelligent signal processing*, 86(2152), 1998.

[36] T. Mori and S. Kai. Noise-induced entrainment and stochastic resonance in human brain waves. *Phys. Rev. Lett.*, 88(218101):1–4, 2002.

[37] N. Mtetwa, L.S. Smith, and A. Hussain. Stochastic resonance and finite resolution in a network of leaky integrate-and-fire neurons. In *Artificial neural networks - ICANN 2002*, pages 117–122, Madrid, Spain, 2002. Springer.

[38] N. Mtetwa, L.S. Smith, and A. Hussain. Stochastic resonance and finite resolutions in a leaky integrate-and-fire neuron. In *ESANN2002: Proceedings of the European Symposium on Artificial Neural Networks, Bruges, Belgium*, pages 343–348, 2002.

[39] D. Petracchi, I.C. Gebeshuber, L.J. DeFelice, and A.V. Holden. Stochastic resonance in biologocal systems. *Chaos, Solutions and Fractals*, 11:1819–1822, 2000.

[40] D. Rousseau, F.B. Duan, and F. Chapeau-Blondeau. Suprathreshold stochastic resonance and noise-enhanced fisher information in arrays of threshold devices. *Phys Rev E*, 2003.

[41] H.S. Seung and H. Sompolinsky. Simple models for reading neuronal population codes. *Proc. Natl. Acad. Sci. USA*, 90:10749–10753, 1993.

[42] G.M. Shepherd. *Neurobiology*. Oxford University Press, 2nd edition, 1988.

[43] T. Shimokawa, A. Rogel, K. Pakdaman, and S. Sato. Stochastic resonance and spike timing in an ensemble of leaky integrate-and-fire neurons model. *Physical Review E*, 59:3461–3470, 1999.

[44] M. Stemmler. A single spike suffices: the simplest form of stochastic resonance in model neurons. *Network: Computation in Neural Systems*, 7(4):687–716, November 1996.

[45] N.G. Stocks. Suprathreshold stochastic resonance in multilevel threshold systems. *Phys. Rev. Lett.*, 84:2310–2314, 2000.

[46] N.G. Stocks. Information transmission in parallel arrays of threshold elements: suprathreshold stochastic resonance. *Phy. Rev. E*, 63(041114):1–9, 2001.

[47] N.G. Stocks, D. Allingham, and R.P. Morse. The application of suprathreshold stochastic resonance to cochlear implant coding. *J. Fluctuation and noise letters*, 2(3):L169–181, 2002.

[48] M. Usher and M. Feingold. Stochastic resonance in the speed of memory retrieval. *Biological Cybernetics*, 83:L11–L16, 2000.

[49] K. Weisenfeld and F. Moss. Stochastic resonance and the benefits of noise: from ice ages to the crayfish and squids. *Nature*, 373:33–36, 1995.

[50] K. Wiesenfeld and F. Jaramillo. Minireview of stochastic resonance. *Chaos*, 8:539–548, 1998.

[51] H.A. Wild and T.A. Busey. Seeing faces in the noise: stochastic activity in perceptual regions of the brain may influence perception of ambiguous stimuli. *Psychonomic Bulletin and Review*, in press, 2003.

[52] Xilinx. *Virtex 2.5 V Field Programmable Gate Arrays*. Xilinx, July 1999.

[53] L. Zalanyi, F. Bazso, and P. Erdi. The effect of synaptic depression on stochastic resonance. *Neurocomputing*, 38-40:459–465, 2001.

[54] F.G. Zeng, O.J. Fu, and R. Morse. Human hearing enhanced by noise. *Brain research*, 869:251–255, 2000.